Metabolic Engineering 18 (2013) 53–59

Contents lists available at SciVerse ScienceDirect

Metabolic Engineering

journal homepage: www.elsevier.com/locate/ymben

Engineered heterologous FPP synthases-mediated *Z,E*-FPP synthesis in *E. coli*

Chonglong Wang [a], Jia Zhou [a], Hui-Jeong Jang [a], Sang-Hwal Yoon [a], Jae-Yean Kim [a], Seung-Goo Lee [b], Eui-Sung Choi [b,*], Seon-Won Kim [a,**]

[a] Division of Applied Life Science (BK21 Program), PMBBRC, Gyeongsang National University, Jinju 660-701, Republic of Korea
[b] Industrial Biotechnology Research Center, KRIBB, Daejeon 305-806, Republic of Korea

ARTICLE INFO

Article history:
Received 24 September 2012
Received in revised form
21 January 2013
Accepted 1 April 2013
Available online 19 April 2013

Keywords:
FPP synthase
Z,E-FPP
Z,E-Farnesol
Protein fusion
Sesquiterpene

ABSTRACT

Production of Z-type farnesyl diphosphate (FPP) has not been reported in *Escherichia coli*. Here we present the fusion enzyme (ILRv) of *E. coli E,E*-FPP synthase (IspA) and *Mycobacterium tuberculosis Z,E*-FPP synthase (Rv1086), which can produce primarily *Z,E*-FPP rather than *E,E*-FPP, the predominant stereoisomer found in most organisms. *Z,E*-farnesol (FOH) was produced from *E. coli* harboring the bottom portion of the MVA pathway and the fusion FPP synthase (ILRv) at a titer of 115.6 mg/L in 2 YT medium containing 1% (v/v) glycerol as a carbon source and 5 mM mevalonate. The *Z,E*-FOH production was improved by 15-fold, compared with 7.7 mg/L obtained from the co-overexpression of separate IspA and Rv1086. The *Z,E*-FPP was not metabolized in native metabolic pathways of *E. coli*. It would be of interest to produce *Z,E*-FPP derived sesquiterpenes from recombinant *E. coli* due to no loss of *Z,E*-FPP substrate in endogenous metabolism of the host strain.

1. Introduction

Isoprenoids are synthesized from 5-carbon (C5) building blocks isopentenyl diphosphate (IPP) and dimethylallyl diphosphate (DMAPP), which are generated either from 2-C-methyl-D-erythritol 4-phosphate (MEP) pathway or mevalonate (MVA) pathway (Bloch et al., 1959; Rohdich et al., 2002). The head-to-tail condensations of IPPs and DMAPP, where the growing hydrocarbon chain of an isoprenoid allylic diphosphate is added to IPP, generate long isoprenyl diphosphates (Lange et al., 2000). The C10 resulting from the condensation of IPP and DMAPP is geranyl diphosphate (GPP), and the addition of a second IPP results in C15 farnesyl diphosphate (FPP) (Fig. 1). These chain elongations can proceed in two possible stereospecific configurations, *E* and *Z*, for the newly formed double bonds. Thus, the stereospecific reaction catalyzed by an FPP synthase results in FPP products with four different potential configurations (*E,E*, *E,Z*, *Z,E* and *Z,Z*) (Thulasiram et al., 2007). The *E*- and *Z*-FPP synthases serve in these stereochemistry reactions, respectively. Most FPP synthases, including *Escherichia coli* IspA, have been characterized as all *E*-double bond forming enzymes, producing *E,E*-FPP (Fujisaki et al., 1990). *E,E*-FPP is known to be utilized for biosynthesis of essential cellular components such as cholesterol, farnesylated proteins, ubiquinones and dolichols in living organisms (Ashby and Edwards, 1990; Clarke, 1992; Matsuoka et al., 1991; Zhang et al., 1993). Few *Z*-FPP synthases have been cloned and identified to date, although long-chain (C40-C200) isoprenyl synthases are found to catalyze *Z*-isoprenyl condensation in general (Bugg and Brandish, 1994). Rv1086 from *Mycobacterium tuberculosis* has been identified as a *Z,E*-FPP synthase catalyzing *Z*-condensation of GPP with IPP (Schulbach et al., 2000).

Sesquiterpenes form a large family of natural products derived from the universal precursor FPP. Most FPP synthases associated with sesquiterpene biosynthesis are *E*-type synthases. *E,E*-FPP is thus assumed as the substrate of sesquiterpene synthases, although it remains to be proven whether *E,E*-FPP is indeed their preferred substrate (Faraldos et al., 2010). In fact, previous studies suggest that *Z*-type (*E,Z*-, *Z,E*- and *Z,Z*-) FPPs may be preferred for the synthesis of some sesquiterpenes. For example, crude enzyme extracts from cotton converted *Z,E*- or Z,Z-FPP to δ-cadinene at a higher efficiency than *E,E*-FPP conversions (Heinstein et al., 1970). The cyclization of *endo*-bergamotene, a sesquiterpene found in tomato, was favored from *Z,E*-FPP rather than *E,E*-FPP owing to stereochemical constraints in the reaction (Coates and Denissen, 1988). More recently, a santalene and bergamotene synthase (SBS) from tomato has been reported to use *Z,Z*-FPP as its sole substrate (Sallaud et al., 2009). Based on these literatures, it is worthwhile to tailor an enzyme to efficiently produce *Z*-type FPPs for industrial sesquiterpene production. We have reported the biosynthesis of *E,E*-farnesol (FOH) from engineered *E. coli* where an exogenous MVA pathway was introduced to supply IPP and DMAPP and IspA was overexpressed to enhance the *E,E*-FPP pool (Wang et al., 2010).

* Corresponding author. Fax: +82 42 860 4489.
** Corresponding author. Fax: +82 55 759 9363.
E-mail addresses: choi4162@kribb.re.kr (E.-S. Choi), swkim@gnu.ac.kr (S.-W. Kim).

1096-7176/$ - see front matter © 2013 Elsevier Inc. All rights reserved.
http://dx.doi.org/10.1016/j.ymben.2013.04.002

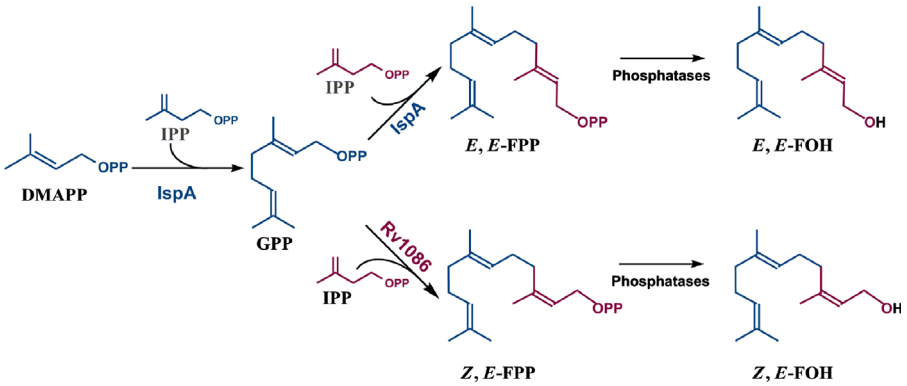

Fig. 1. Scheme of *E,E*- and *Z,E*-FOH synthesis pathway. The IPP and DMAPP precursors are synthesized by either the MEP or MVA pathway. *E,E*-FPP is synthesized by IspA through the condensation of 1 DMAPP and 2 IPPs. Rv1086 catalyzes the condensation of GPP and IPP to form *Z,E*-FPP. Abbreviations of the pathway intermediates are as follows: DMAPP, dimethylallyl pyrophosphate; IPP, isopentenyl pyrophosphate; GPP, geranyl pyrophosphate; *E,E*-FPP, *E,E*-farnesyl pyrophosphate; *Z,E*-FPP, *Z,E*-farnesyl pyrophosphate; *E,E*-FOH, *E,E*-farnesol; *Z,E*-FOH, *Z,E*-farnesol. The enzyme abbreviations are as follows: IspA, *E,E*-FPP synthase; Rv1086, *Z,E*-FPP synthase of *M. tuberculosis*; phosphatases, unknown endogenous phosphatases of *E. coli*.

It was suggested that *E,E*-FOH formation relies on endogenous phosphatases, which usually have broad substrate specificities and can hydrolyze a range of phosphoesters including FPP (Touze et al., 2008; Wang et al., 2011a). Therefore, it is potentially possible to synthesize Z-type FOHs from engineered *E. coli* harboring *Z*-type FPP synthases instead of IspA. In this paper, we present the fusion enzyme (ILRv) of *E. coli E,E*-FPP synthase (IspA) and *Mycobacterium tuberculosis Z,E*-FPP synthase (Rv1086) which can dominantly produce *Z,E*-FPP rather than *E,E*-FPP in *E. coli*.

2. Materials and methods

2.1. Strains and growth conditions

Strains used in this study are listed in Table 1. *E. coli* DH5α was used as a host strain for plasmids construction and FOH production. The FPP synthase gene (*ispA*) was deleted by Red/ET recombination (Gene Bridges GmbH, Germany) to create *E. coli* DH5α Δ*ispA*, which was used as a host strain for growth rescue study. The kanamycin resistance cassette for the *ispA* deletion was amplified from *E. coli* SF7N genomic DNA (Fujisaki et al., 2005) using the primers DispA-F and DispA-R (Table 1). *E. coli* BL21 (DE3) was used as a host strain for protein purification.

E. coli DH5α was grown at 37 °C in 2 YT (16 g/L tryptone, 10 g/L yeast extract, and 5 g/L NaCl) medium for plasmid constructions. *E. coli* strains used for FOH production and growth rescue study were cultivated at 29 °C in 2 YT medium containing 1% (v/v) glycerol and 0.1 mM IPTG. Mevalonate was supplied at 5 mM for culture of recombinant *E. coli* harboring pSSN12Didi plasmid, which contained the bottom portion of the MVA pathway (Yoon et al., 2009, 2006). The decane-overlaid two-phase culture for FOH production was performed as in the previous report (Wang et al., 2010). All cultivations were performed in duplicate. *E. coli* BL21 (DE3) was grown at 22 °C in LB (10 g/L tryptone, 5 g/L yeast extract, and 10 g/L NaCl) medium for protein purification. Antibiotics of ampicillin (100 μg/ml), chloramphenicol (50 μg/ml) and kanamycin (50 μg/ml) were added as required.

2.2. Construction of plasmids

Standard molecular biology techniques were used to carry out plasmid construction (Sambrook and Russell, 2001). The *Rv1086* gene encoding *Z*-type FPP synthase was amplified from the genomic DNA of *Mycobacterium tuberculosis* H37Rv (ATCC 25177D-5) through PCR reaction with primers Rv1086-F1 and Rv1086-R. The PCR product was digested with *Bam*HI and *Xho*I and cloned into the *Bam*HI/*Sal*I sites of pTrc99A vector to create the pTRv1086 plasmid. The pTispARv1086 plasmid was constructed by integrating the PCR product of the *Rv1086* gene amplified with primers Rv1086-F2 and Rv1086-R into the *Bam*HI/*Sal*I sites of pTispA (Wang et al., 2010). For the construction of the pTispALRv1086 plasmid, the *Rv1086* gene was introduced into *Bam*HI/*Sal*I sites of pTispAL where the stop codon (TAA) of *ispA* gene was replaced with an oligonucleotide encoding a $(GGGGS)_2$ peptide linker (Wang et al., 2011b). For the construction of the pETispALRv1086 plasmid, the *ispALRv1086* fragment cut from pTispALRv1086 by *Eco*RI and *Hind*III was inserted into the *Eco*RI/*Hind*III sites of pET28a (Novagen, Darmstadt, Germany). The plasmids and PCR primers used in this study are listed in Table 1.

2.3. Site-directed mutagenesis

Mutants of ispALRv1086 were generated using the PCR-based QuickChange site-directed mutagenesis kit (Stratagene, Santa Clara, CA) according to the manufacturer's instructions. Primers ispA^{S80F}-F and ispA^{S80F}-R were used to generate ispA^{S80F}LRv1086. Primers Rv1086^{V107W}-F and Rv1086^{V107W}-R were used to generate ispALRv1086^{V107G}. Each of the mutated ispALRv1086 was sequenced by Solgent Corp. (Daejeon, Korea) to ensure that only the appropriated mutations had been incorporated.

2.4. Analysis of FOH products

FOH production was quantified by gas chromatography (GC) as described previously (Wang et al., 2010). Briefly, a gas chromatograph (Agilent Technologies 7890A) equipped with a flame ionization detector (FID) and an autosampler was used. Samples were injected into HP-INNOWAX column (19091 N-133, 30 m in length, 0.25 mm in internal diameter, and 250 μm in film thickness) at a split ratio of 1:10. The oven temperature was initiated at 50 °C for 1 min and increased at rates of 25 °C/min to 150 °C and then 10 °C/min to 250 °C where it was held for 1 min. Nitrogen was used as the carrier gas with an inlet pressure of 39 *psi*. The detector was maintained at 260 °C. Full mass spectra were generated by scanning m/z range within 35–300 for FOH identification. The *Z,E*-FOH and *E,E*-FOH were identified comparing mass spectra and retention time with the available authentic standards (Supplementary Fig. S1). Quantification of *Z,E*-FOH and *E,E*-FOH was carried out using a standard curve of *E,E*-FOH (Sigma-Aldrich, St. Louis, MO) (Supplementary Fig. S2).

2.5. SDS-PAGE and native-PAGE analyses of IspA-Rv1086 (ILRv) fusion protein

The IspA-Rv1086 (ILRv) fusion protein was purified from *E. coli* BL21 (DE3) harboring pETispALRv086. The culture was grown at

Table 1
Strains, plasmids and primers used in this study.

Names	Descriptions	References
***E. coli* strains**		
BL21 (DE3)	*F*$^-$, *ompT*, *hsdS*$_B$(r_B^-, m_B^-), *dcm*, *gal*, λ(DE3)	Novagen
SF7N	*F*$^-$, λ$^-$, IN(*rrnD-rrnE*)1, *rph*-1, Δ*ispA*::FRT-*Kan*-FRT	(Fujisaki et al., 2005)
DH5α	*F*$^-$, *fhuA*2, Δ*(argF-lacZ)U*169, *phoA*, *glnV*44, Φ80 Δ*(lacZ)M*15, *gyrA*96, *recA*1, *relA*1, *endA*1, *thi*-1, *hsdR*17(r_K^-, m_K^+)	ATCC
SN-C	DH5α containing pSSN12Didi and pTrc99A	This study
SN-Rv	DH5α containing pSSN12Didi and pTRv1086	This study
SN-I	DH5α containing pSSN12Didi and pTispA	This study
SN-IRv	DH5α containing pSSN12Didi and pTispARv1086	This study
SN-ILRv	DH5α containing pSSN12Didi and pTispALRv1086	This study
SN-I^{S80F}LRv	DH5α containing pSSN12Didi and pTispA^{S80F}LRv1086	This study
SN-ILRv^{V107G}	DH5α containing pSSN12Didi and pTispALRv1086^{V107G}	This study
DH5α Δ*ispA*	DH5α Δ*ispA*::FRT-*Kan*-FRT	This study
WT-C	DH5α containing pTrc99A	This study
MU-C	DH5α Δ*ispA* containing pTrc99A	This study
MU-I	DH5α Δ*ispA* containing pTispA	This study
MU-Rv	DH5α Δ*ispA* containing pTRv1086	This study
MU-ILRv	DH5α Δ*ispA* containing pTispALRv1086	This study
MU-I^{S80F}LRv	DH5α Δ*ispA* containing pTispA^{S80F}LRv1086	This study
Plasmids		
pTrc99A	P_{trc}; *lacI*^{q}; pBR322 ori; *Amp*^{R}	
pTRv1086	P_{trc}:: *Rv1086*; *lacI*^{q}; pBR322 ori; *Amp*^{R}	This study
pTispA	P_{trc}:: *ispA*; *lacI*^{q}; pBR322 ori; *Amp*^{R}	(Wang et al., 2010)
pTispARv1086	P_{trc}:: *ispA*, *Rv1086*; *lacI*^{q}; pBR322 ori; *Amp*^{R}	This study
pTispALRv1086	P_{trc}:: *ispALRv1086*; *lacI*^{q}; pBR322 ori; *Amp*^{R}	This study
pTispA^{S80F}LRv1086	P_{trc}:: *ispA*^{S80F}*LRv1086*; *lacI*^{q}; pBR322 ori; *Amp*^{R}	This study
pTispALRv1086^{V107G}	P_{trc}:: *ispALRv1086*^{V107G}; *lacI*^{q}; pBR322 ori; *Amp*^{R}	This study
pETispALRv1086	P_{T7}:: *his6 tag-ispA*^{S80F}*LRv1086*; *lacI*; pBR322 ori; *Kan*^{R}	This study
pSSN12Didi	P_{lac}:: *mvaK1*, *mvaK2*, *mvaD*, *idi*; p15A ori; *Cm*^{R}	(Yoon et al., 2006; Yoon et al., 2009)
Primers		
Rv1086-F1	TAGGATCC**ATG**GAGATCATCCCGCCGCG	This study
Rv1086-F2	TGGATCC*AGGAGGTAATAAACC***ATG**GAGATCATCCCGCCGCG	This study
Rv1086-R	ATC*TCGAG***TTA**CCTGCCGTAGCTGCGATGC	This study
ispA^{S80F}-F	GAGTGTATCCACGCTTACTTTTTAATTCATGATGATTTACCG	This study
ispA^{S80F}-R	AAAGTAAGCGTGGATACACTCAACGGCGGCAGC	This study
Rv1086 ^{V107G}-F	CATCACCGATGGCGTGGAAGAGATCTGCGC	This study
Rv1086 ^{V107G}-F	CTTCCACGCCATCGGTGATGATCTCGATG	This study
DispA-F	GCGTACAAATTCTGCTGTCTGAC	This study
DispA-R	CAACAGTCGTAACTCCTGGGTG	This study

Note: Start codons or stop codon are in bold, enzyme sites are underlined, and ribosome binding site is in italics.

37 °C to OD600 = 0.6 to 0.8 before inducing with 0.1 mM IPTG and dropping the temperature to 22 °C. The culture was grown for an additional 20 h and then harvested by centrifugation and disrupted by sonication in 20 mM phosphate buffer (pH 7.9) containing 400 mM NaCl and 10 mM imidazole. Soluble His-tagged proteins were purified by a nickel-nitrilotriacetic acid-agarose column (Invitrogen, Carlsbad, CA). The purified ILRv protein was analyzed on 12% SDS-polyacrylamide gel electrophoresis (SDS-PAGE) using Bio-Rad (Hercules, CA) mini gel electrophoresis apparatus following the Laemmli's procedure (Cluis et al., 2011). To determine oligomers formed by the purified ILRv protein, Native-PAGE was used to separate protein complex at 4 °C in the absence of SDS. Gels were visualized by Coomassie-blue staining.

3. Results and discussions

3.1. Expression of Rv1086 results in Z,E-FPP synthesis

We have previously speculated that endogenous phosphatases can hydrolyze FPP to FOH in *E. coli* when intracellular FPP is elevated to a high level. Indeed, *E,E*-FOH formation was triggered by overexpression of IspA and introduction of a well-performing MVA pathway to enhance the FPP synthesis (Wang et al., 2010). We thus assumed that the improvement of the synthesis of *Z*-type FPP can result in the production of Z-type FOH in *E. coli*. To test this hypothesis, *M. tuberculosis Rv1086* gene encoding a *Z*-type FPP synthase was co-expressed in *E. coli* with the bottom portion of MVA pathway encoded in pSSN12Didi. As expected, the functional expression of Rv1086 resulted in *Z,E*-FOH formation in *E. coli* SN-Rv supplemented with 5 mM mevalonate, while the strain overexpressing *E*-tpye FPP synthase (*E. coli* SN-I) produced *E,E*-FOH as its sole product (Fig. 2A, B and Supplementary Fig. S3). Since Rv1086 is able to catalyze only the single step reaction of GPP to FPP and cannot use DMAPP as a substrate, the formation of *Z,E*-FOH reflecting *Z,E*-FPP synthesis indicates that GPP is available to Rv1086 even in *E. coli* with no designated endogenous GPP synthase.

The production of monoterpene in winemaking *Saccharomyces cerevisae* has been reported previously (Ma et al., 2011; Ozaydin et al., 2013). FPP synthase of *S. cerevisae* is noted to contribute a monoterpene production by releasing GPP (Fischer et al., 2011), although it is usually thought that GPP is not released from the catalytic site, and is entirely converted to FPP. Therefore, the endogenous FPP synthase (IspA) would also be the most likely player of GPP synthesis in *E. coli*. Moreover, the considerable amount (39.5% of total FOH production) of *Z,E*-FOH production from *E. coli* SN-Rv hinted us to reconsider the general concept of the directed synthesis of FPP in IspA. We hypothesized that the endogenous IspA releases GPP after the first condensation reaction

of DMAPP and IPP, and subsequently takes up the GPP for the second condensation reaction of GPP and IPP for FPP formation. The native MEP pathway supplies *E. coli* with DMAPP and IPP at a low flux and the released GPP from IspA can be quickly recruited again, which may hide the fact of GPP release from IspA before the second condensation reaction. However, the release was unveiled when sufficient DMAPP and IPP were supplied through the additional MVA pathway overexpressed in cells. To support this hypothesis, we observed geraniol synthesized from GPP in cultures of strain *E. coli* SN-Rv and *E. coli* SN-C, but not in *E. coli* SN-I and *E. coli* IRv (Supplementary Fig. S4). Production of geraniol offers strong circumstantial evidence that GPP is released by IspA in the engineered strains. The GPP accumulation in the cells was also observed by UPLC-MS/MS (data not shown here) and overall isoprenyl intermediates analysis is going further. Thus, *Z,E*-FPP synthesis is most likely the result of Rv1086 competing with IspA for the GPP substrate released from IspA.

3.2. Re-direction of GPP flux to Z,E-FPP synthesis by IspA-Rv1086 fusion chimera

It is interesting to note that the total (*E,E*- and *Z,E*-) FOH production in *E. coli* SN-Rv (75.3 mg/L) was significantly lower than that in *E. coli* SN-I (128.0 mg/L) (Fig. 2B). As GPP is supplied from IspA, the available amount of GPP for FPP synthesis could be limited in *E. coli* SN-Rv with only a single copy of *ispA* gene on its chromosome, compared to *E. coli* SN-I with multiple copies of *ispA* gene on the pTispA plasmid. Co-overexpression of IspA and Rv1086 in *E. coli* SN-IRv resulted in a total FOH production (118.2 mg/L) comparable to that of *E. coli* SN-I. It also resulted in a significant decrease in *Z,E*-FOH production (7.7 mg/L), just to 6.5% of the total FOH production (Fig. 2B). This suggests that the increase of GPP availability for *Z,E*-FPP synthesis is compromised by GPP consumption by IspA when it is overexpressed in *E. coli* SN-IRv. We thus hypothesized that the competition between IspA and Rv1086 is influenced by both the relative amount of each enzyme and the distance between the GPP substrate and the enzymes (Fig. 2C). In the case of *E. coli* SN-Rv, RV1086 has an advantage over IspA in the competition for GPP substrate due to its higher enzyme level resulting from plasmid-based expression, whereas in *E. coli* SN-IRv, IspA is highly competitive over Rv1086 due to its inherent proximity to GPP.

An IspA-Rv1086 (ILRv) fusion protein was constructed with a glycine–serine linker as an approach to facilitate the competition of Rv1086 for GPP against IspA. The prerequisites of fusion protein application to metabolic engineering are soluble expression of the chimeric enzyme and maintenance of both enzymatic activities (Albertsen et al., 2011). The solubility of the chimeric ILRv was thus probed in an SDS-PAGE analysis (Fig. 3A). The apparent molecular weight of monomeric ILRv was larger than its theoretical molecular weight (63.2 KDa), which is consistent with the observation of the individual proteins (Fujisaki et al., 1990; Schulbach et al., 2001). Both IspA and Rv1086 are Mg^{2+}-dependent homodimeric enzymes, although there is no structure similarity between the two prenyltransferases (Hosfield et al., 2004; Wang et al., 2008). IspA activity is totally dependent on the homodimer formation (Koyama et al., 2000). We observed the ILRv chimera migrating at approximately130 kDa as a major band and 260 kDa as a minor band in native-PAGE (Fig. 3B). It suggested that the ILRv was generally present in a dimer form, and also likely in a tetramer form (Fig. 3C). Moreover, the glycine–serine linker, although it will occur less likely in nature, can be fully extended ($\Phi = 180^\circ$, $\Psi = 180^\circ$) up to approximately 3.6 nm, which is comparable to an average diameter (5 nm) of proteins in *E. coli* (http://redpoll.pharmacy.ualberta.ca/CCDB/). The length can allow the Rv1086 domain of the fusion chimera to move freely around the IspA domain (Fig. 3D). These data indicate that IspA and RV1086 are successfully fused by the glycine–serine linker, and that the solubility of the chimeric protein is maintained in *E. coli*.

We subsequently tested the FPP synthase activity of the ILRv chimera in an *ispA* deletion strain, *E. coli* DH5α Δ*ispA*. The *ispA* gene is known to be very important for maintenance of proper growth in *E. coli* (Fujisaki et al., 2005); consistent with this, a severe retardation of cell growth was observed in *E. coli* MU-C (Fig. 4). Plasmid-mediated expression of either IspA (MU-I) or the chimera ILRv (MU-ILRv) restored the growth rate, demonstrating that both proteins could complement the *ispA* mutant. These results indicate that FPP synthase activity of IspA was retained in the ILRv fusion chimera. Expression of Rv1086 (MU-Rv) failed to rescue the damaged growth, presumably because Rv1086 cannot utilize DMAPP as the allylic substrate for FPP synthesis (Schulbach et al., 2001). To probe that there is no steric hindrance between two fusion partners, we generated a variant fusion chimera, IspA-Rv1086^{V107G} (ILRv^{V107G}). The V107G mutation is known to inactivate Rv1086, although Rv1086^{V107G} is still expressed in soluble form (Wang et al., 2008). *E. coli* SN-ILRv1086 ^{V107G} behaved just as *E. coli* SN-I, with a comparable *E,E*-FOH production and no *Z,E*-FOH (Fig. 2B). It indicates that IspA domain of the ILRv fusion chimera can function as the free IspA.

Finally, *E. coli* SN-ILRv harboring the ILRv fusion chimera successfully produced 115.6 mg/L of *Z,E*-FOH, which was 80.7% of the total FOH production (143.3 mg/L) (Fig. 2B). The fusion of IspA and Rv1086 (SN-ILRv) did increase the availability of GPP to Rv1086 and resulted in a more favorable production of *Z,E*-FPP synthesis relative to the overexpression of Rv1086 alone (Fig. 2A, B). If there was no contribution from chromosomal IspA to *E,E*-FPP synthesis, the *Z,E*-FOH production using ILRv could be obtained at more than 80.7%. Thus, the spatial neighboring arrangement of Rv1086 and IspA allows Rv1086 to effectively compete for GPP against IspA (Fig. 2C). It is also noted that the affinities of Rv1086 for GPP (K_M, 7.8 μM) and IPP (K_M, 4.5 μM) are comparable to those of IspA (Supplementary Table. S1) (Ambo et al., 2008; Fujisaki et al., 1986), and turnover numbers (k_{cat}) of IspA and Rv1086 can play a major role in the competing use of GPP and IPP substrates rather than their K_M properties. The biased *Z,E*-FPP synthesis from the ILRv chimera thus imply that Rv1086 has a faster rate of turnover than IspA. GPP synthases have been identified from some of plants and bacteria such as *Abies grandis*, *Arabidopsis thaliana* and *M. tuberculosis* (Bouvier et al., 2000; Burke and Croteau, 2002; Mann et al., 2011). However, the use of plant GPP synthases has not been successful to date in achieving reasonable levels of monoterpene production in *E. coli* (Carter et al., 2003). Protein engineering of FPP synthase for GPP synthesis also suffers from a reduction in enzyme activity (Reiling et al., 2004) (See also Section 3.3). The *Z,E*-FPP synthesis by IspA-Rv1086 fusion protein suggests an attractive alternative way for GPP supply, which can be employed for monoterpene production in a host with no available efficient GPP synthase, if a monoterpene synthase is successfully fused with IspA like as the IspA-Rv1086 fusion protein.

3.3. Z,E-FPP is not metabolized for essential isoprenoids in E. coli

E,E-FPP lies at an important multiple branch point in the isoprenoid pathway as a precursor for synthesis of essential isoprenoid compounds such as quinones and lipid carriers. Thus, the *E,E*-FPP flux towards formation of endogenous isoprenoids is a metabolic waste in production of interesting sesquiterpenes. The waste flux to endogenous isoprenoids may even be increased in cells with an enhanced synthesis of *E,E*-FPP for mass production of target sesquiterpenes. If *Z,E*-FPP is not metabolized for endogenous isoprenoid formation in *E. coli*, it can be utilized solely for the synthesis of target sesquiterpenes. To address whether *Z,E*-FPP is used for synthesis of endogenous

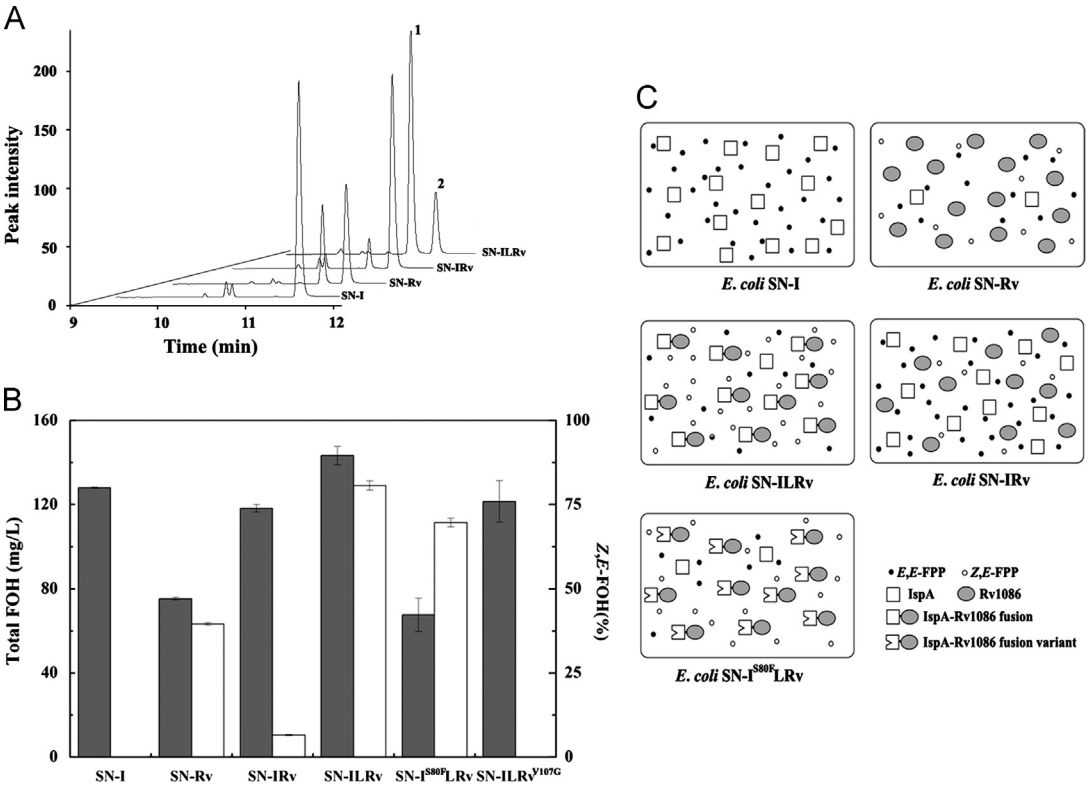

Fig. 2. Characterization of *Z,E*-FOH formation in recombinant *E. coli* expressing Rv1086 of *M. tuberculosis* (A) GC chromatographs of extracted FOH from recombinant *E. coli* strains. Peak 1 and Peak 2 indicate *Z,E*-FOH and *E,E*-FOH, respectively. (B) Total FOH production and relative *Z,E*-FOH production in recombinant *E. coli* strains. The closed and open bars represent total FOH production and *Z,E*-FOH proportion, respectively. Error bars represent the standard deviation of two biological replicates. (**C**) Scheme of spatial location of IspA and Rv1086 and their products in cells.

isoprenoids, we generated another variant fusion chimera, IspA^{S80F}-Rv1086 (I^{S80F}LRv). The S80F mutation in IspA^{S80F} has been known to make the IspA mutant synthesize GPP only, although the S80F mutation impairs the catalytic behavior of IspA (Narita et al., 1999; Reiling et al., 2004). Thus, the variant fusion chimera, I^{S80F}LRv would produce *Z,E*-FPP specifically and no *E,E*-FPP. The functional expression of I^{S80F}LRv was verified by *Z,E*-FOH formation in *E. coli* SN- I^{S80F}LRv (Fig. 2B). Owing to the low capacity in stage of GPP synthesis, *E. coli* SN- I^{S80F}LRv produced less FOH than the *E. coli* SN- ILRv, but as much as that of *E. coli* SN-Rv. It was noteworthy that the *Z,E*-FOH proportion was increased by 1.7-fold when comparing to that of *E. coli* SN-Rv. The increased relative *Z,E*-FOH production supports that I^{S80F}LRv functions to synthesize *Z,E*-FPP (Fig. 2C). Next, the variant fusion chimera was introduced into *E. coli* Δ*ispA* to see whether *Z,E*-FPP complements the defective growth in the mutant. If the growth retardation shown in *E. coli* MU-C is not observed in *E. coli* MU-I^{S80F}LRv, it would suggest that *Z,E*-FPP can be used for the buildup of essential endogenous isoprenoids in *E. coli*. The result is that cell growth of *E. coli* Δ*ispA* was not restored by the expression of I^{S80F}LRv, and the growth of *E. coli* MU-I^{S80F}LRv was even worse than *E. coli* MU-C (Fig. 4). It is therefore concluded that *Z,E*-FPP is not metabolized for the synthesis of essential isoprenoids, resulting in the poorer growth rate. Both octaprenyl diphosphate and undecaprenyl diphosphate synthases are known to have a slight activity of FPP synthesis from the condensation of IPPs and short chain allylic diphosphates (DMAPP and GPP), to which the survival or slow growth of *ispA* deletion mutants could be attributed (Fujisaki et al., 1986, 2005). The coupling of IPP and DMAPP (and GPP) to the non-metabolizable *Z,E*-FPP may aggravate the poor cell growth in *E. coli* MU-I^{S80F}LRv and Mu-Rv than Mu-C.

Sesquiterpene synthases catalyze the buildup of alicyclic precursor FPP into structurally diverse sesquiterpene products. There is a direct correspondence between the absolute stereochemical configuration of the sesquiterpene products and the inferred conformation of the precursor FPP (Cane, 1985). To give rise to a diverse of FPP conformations, *E,E*-FPP undergoes multi-steps of electrophilic cyclizations, rotations and rearrangements (Davis and Croteau, 2001). However, such conformations sometime can be easily built from *Z*-type FPP. It suggests that some sesquiterpene synthases can take up or prefer *Z*-type FPP as a substrate, and *Z,E*-FPP is indeed cyclized by cadinene synthase, *epi*-aristolochene synthase, *etc.* (Faraldos et al., 2012, 2010; Lopez-Gallego et al., 2010). The *epi*-aristolochene synthase possesses an almost identical catalytic efficiency (k_{cat}/K_M) for both native *E,E*-FPP and alternative *Z,E*-FPP substrates (Noel et al., 2010). If a novel sesquiterpene synthase either newly characterized or engineered can effectively catalyze *Z,E*-FPP to an interesting sesquiterpene product, there will be some advantages over starting from *E,E*-FPP such as no loss of *Z,E*-FPP flux to endogenous isoprenoids synthesis and no endogenous feed-back regulations on *Z,E*-FPP synthesis.

4. Conclusion

Metabolic engineering of microorganisms for the production of value-added chemicals holds great promise for industrial applications (Cluis et al., 2011; Redding-Johanson et al., 2011; Scalcinati et al., 2012). Enzymatic processes are known to catalyze reactions with an intrinsic stereospecificity that is not easy to achieve through chemical synthesis (Yu et al., 2005). In this study, we engineered an FPP synthase by fusion of *M. tuberculosis* Rv1086 and *E. coli* IspA to produce *Z,E*-FPP, a promising substrate for the synthesis of sesquiterpenes. By this approach, the engineered strain *E. coli* SN-IRv produced 115.6 mg/L of *Z,E*-FOH, a 15-fold increase over the co-overexpression of separate IspA and Rv1086. The stereospecific formation of *Z,E*-FOH from *Z,E*-FPP also suggests an exquisite way to analyze FPP stereoisomers generated from the engineered strains.

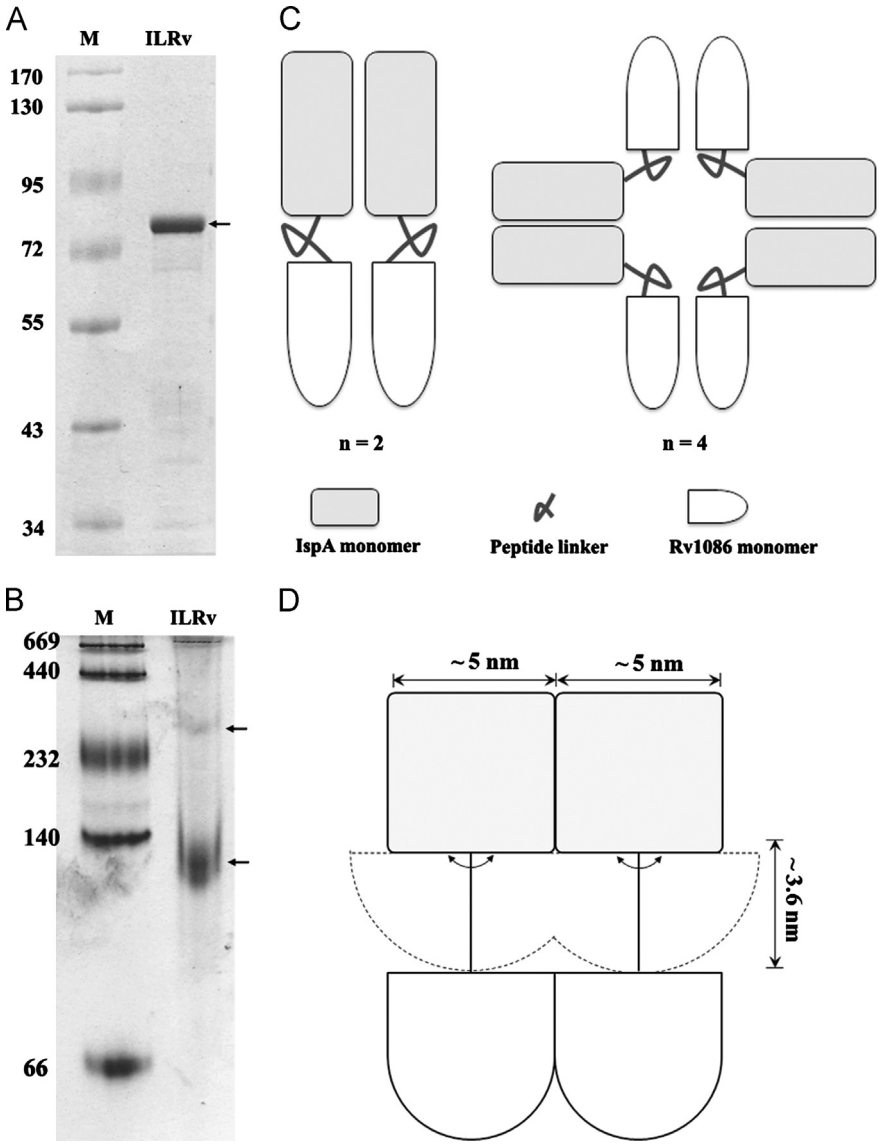

Fig. 3. Analyses of purified IspA-Rv1086 (ILRv) fusion protein. (**A**) SDS-PAGE analysis. The left lane (M) shows the molecular weight ladder. The Purified ILRv protein is arrowed. (B) Native-PAGE analysis. The left lane (M) shows the molecular weight ladder. Oligomers formed by ILRv protein are arrowed. (C) Possible structural configurations of the fusion protein. The $n=2$ and 4 indicate the number of ILRv monomer. (D) Motion scheme of flexible glycine–serine linker in the ILRv dimer.

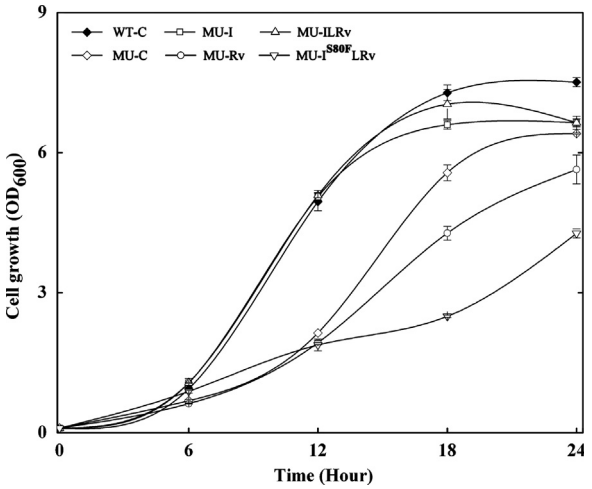

Fig. 4. Complementation of *E. coli* DH5α Δ*ispA* cell growth by IspA, Rv1086 and their fusion proteins. Strains are listed in Table 1. Error bars represent the standard deviation of two biological replicates.

Minimizing loss of precursor metabolites is a prerequisite in metabolic engineering approaches (Ozaydin et al., 2013). Our results indicate that *Z,E*-FPP is not metabolized to non-FOH products in *E. coli*. The utilization of *Z,E*-FPP for sesquiterpene production can be an advantageous over the use of *E,E*-FPP as a precursor. The entire MVA pathway has been successfully engineered for supply of DMAPP and IPP from a simple and inexpensive carbon source such as glycerol (Ma et al., 2011; Martin et al., 2003; Yoon et al., 2009). The application of IspA-Rv1086 fusion protein combined with the engineered MVA pathway can be a good platform for the overproduction of sesquiterpenes utilizing *Z,E*-FPP, when appropriate sesquiterpene synthases are introduced into the host.

Acknowledgments

This work was supported by a Grant (NRF-2010-C1AAA001-0029084) from the National Research Foundation, the Intelligent Synthetic Biology Center of Global Frontier Project funded by the MEST (2011–0031964), and a Grant from the Next-Generation

BioGreen 21 Program, (SSAC Grant#: PJ0081842012), RDA, Korea. Jia Zhou and Hui-Jeong Jang are supported by scholarships from the BK21 Program, MEST, Korea.

Appendix A. Supporting information

Supplementary data associated with this article can be found in the online version at http://dx.doi.org/10.1016/j.ymben.2013.04.002.

References

Albertsen, L., Chen, Y., Bach, L.S., Rattleff, S., Maury, J., Brix, S., Nielsen, J., Mortensen, U.H., 2011. Diversion of flux toward sesquiterpene production in Saccharomyces cerevisiae by fusion of host and heterologous enzymes. Appl Environ. Microbiol. 77, 1033–1040.

Ambo, T., Noike, M., Kurokawa, H., Koyama, T., 2008. Cloning and functional analysis of novel short-chain cis-prenyltransferases. Biochem. Biophys. Res. Commun. 375, 536–540.

Ashby, M.N., Edwards, P.A., 1990. Elucidation of the deficiency in two yeast coenzyme Q mutants. Characterization of the structural gene encoding hexaprenyl pyrophosphate synthetase. J. Biol. Chem. 265, 13157–13164.

Bloch, K., Chaykin, S., Phillips, A.H., De Waard, A., 1959. Mevalonic acid pyrophosphate and isopentenylpyrophosphate. J. Biol. Chem. 234, 2595–2604.

Bouvier, F., Suire, C., d'Harlingue, A., Backhaus, R.A., Camara, B., 2000. Molecular cloning of geranyl diphosphate synthase and compartmentation of monoterpene synthesis in plant cells. Plant J. 24, 241–252.

Bugg, T.D., Brandish, P.E., 1994. From peptidoglycan to glycoproteins: common features of lipid-linked oligosaccharide biosynthesis. FEMS Microbiol. Lett. 119, 255–262.

Burke, C., Croteau, R., 2002. Geranyl diphosphate synthase from Abies grandis: cDNA isolation, functional expression, and characterization. Arch. Biochem. Biophys. 405, 130–136.

Cane, D.E., 1985. Isoprenoid biosynthesis. stereochemistry of the cyclization of allylic pyrophosphates. Acc. Chem. Res. 18, 220–226.

Carter, O.A., Peters, R.J., Croteau, R., 2003. Monoterpene biosynthesis pathway construction in *Escherichia coli*. Phytochemistry 64, 425–433.

Clarke, S., 1992. Protein isoprenylation and methylation at carboxyl-terminal cysteine residues. Annu. Rev. Biochem. 61, 355–386.

Cluis, C.P., Ekins, A., Narcross, L., Jiang, H., Gold, N.D., Burja, A.M., Martin, V.J., 2011. Identification of bottlenecks in *Escherichia coli* engineered for the production of CoQ(10). Metab. Eng. 13, 733–744.

Coates, R.M., Denissen, J.F., 1988. identifiaction of alpha-santalenoic and endo-beta-bergamotenoic acids as moth oviposition stimulants from wild tomato leaves. J. Org. Chem. 52, 2186–2192.

Davis, E.M., Croteau, R., 2001. Cyclization enzymes in the biosynthesis of monoterpenes, sesquiterpenes, and diterpenes. Top. Curr. Chem. 209, 54–95.

Faraldos, J.A., Miller, D.J., Gonzalez, V., Yoosuf-Aly, Z., Cascon, O., Li, A., Allemann, R. K., 2012. A 1,6-ring closure mechanism for (+)-delta-cadinene synthase? J. Am. Chem. Soc. 134, 5900–5908.

Faraldos, J.A., O'Maille, P.E., Dellas, N., Noel, J.P., Coates, R.M., 2010. Bisabolyl-derived sesquiterpenes from tobacco 5-epi-aristolochene synthase-catalyzed cyclization of (2Z,6E)-farnesyl diphosphate. J. Am. Chem. Soc. 132, 4281–4289.

Fischer, M.J., Meyer, S., Claudel, P., Bergdoll, M., Karst, F., 2011. Metabolic engineering of monoterpene synthesis in yeast. Biotechnol. Bioeng. 108, 1883–1892.

Fujisaki, S., Hara, H., Nishimura, Y., Horiuchi, K., Nishino, T., 1990. Cloning and nucleotide sequence of the ispA gene responsible for farnesyl diphosphate synthase activity in *Escherichia coli*. J. Biochem. 108, 995–1000.

Fujisaki, S., Nishino, T., Katsuki, H., 1986. Isoprenoid synthesis in *Escherichia coli*. Separation and partial purification of four enzymes involved in the synthesis. J. Biochem. 99, 1327–1337.

Fujisaki, S., Takahashi, I., Hara, H., Horiuchi, K., Nishino, T., Nishimura, Y., 2005. Disruption of the structural gene for farnesyl diphosphate synthase in *Escherichia coli*. J. Biochem. 137, 395–400.

Heinstein, P.F., Herman, D.L., Tove, S.B., Smith, F.H., 1970. Biosynthesis of gossypol. Incorporation of mevalonate-2-14C and isoprenyl pyrophosphates. J. Biol. Chem. 245, 4658–4665.

Hosfield, D.J., Zhang, Y., Dougan, D.R., Broun, A., Tari, L.W., Swanson, R.V., Finn, J., 2004. Structural basis for bisphosphonate-mediated inhibition of isoprenoid biosynthesis. J. Biol. Chem. 279, 8526–8529.

Koyama, T., Gotoh, Y., Nishino, T., 2000. Intersubunit location of the active site of farnesyl diphosphate synthase: reconstruction of active enzymes by hybrid-type heteromeric dimers of site-directed mutants. Biochemistry 39, 463–469.

Lange, B.M., Rujan, T., Martin, W., Croteau, R., 2000. Isoprenoid biosynthesis: the evolution of two ancient and distinct pathways across genomes. Proc. Natl. Acad. Sci. USA 97, 13172–13177.

Lopez-Gallego, F., Agger, S.A., Abate-Pella, D., Distefano, M.D., Schmidt-Dannert, C., 2010. Sesquiterpene synthases Cop4 and Cop6 from Coprinus cinereus: catalytic promiscuity and cyclization of farnesyl pyrophosphate geometric isomers. Chembiochem 11, 1093–1106.

Ma, S.M., Garcia, D.E., Redding-Johanson, A.M., Friedland, G.D., Chan, R., Batth, T.S., Haliburton, J.R., Chivian, D., Keasling, J.D., Petzold, C.J., Lee, T.S., Chhabra, S.R., 2011. Optimization of a heterologous mevalonate pathway through the use of variant HMG-CoA reductases. Metab. Eng. 13, 588–597.

Mann, F.M., Thomas, J.A., Peters, R.J., 2011. Rv0989c encodes a novel (E)-geranyl diphosphate synthase facilitating decaprenyl diphosphate biosynthesis in *Mycobacterium tuberculosis*. FEBS Lett. 585, 549–554.

Martin, V.J., Pitera, D.J., Withers, S.T., Newman, J.D., Keasling, J.D., 2003. Engineering a mevalonate pathway in *Escherichia coli* for production of terpenoids. Nat. Biotechnol. 21, 796–802.

Matsuoka, S., Sagami, H., Kurisaki, A., Ogura, K., 1991. Variable product specificity of microsomal dehydrodolichyl diphosphate synthase from rat liver. J. Biol. Chem. 266, 3464–3468.

Narita, K., Ohnuma, S., Nishino, T., 1999. Protein design of geranyl diphosphate synthase. Structural features that define the product specificities of prenyltransferases. J. Biochem. 126, 566–571.

Noel, J.P., Dellas, N., Faraldos, J.A., Zhao, M., Hess Jr., B.A., Smentek, L., Coates, R.M., O'Maille, P.E., 2010. Structural elucidation of cisoid and transoid cyclization pathways of a sesquiterpene synthase using 2-fluorofarnesyl diphosphatesACS Chem. Biol. 5, 377–392.

Ozaydin, B., Burd, H., Lee, T.S., Keasling, J.D., 2013. Carotenoid-based phenotypic screen of the yeast deletion collection reveals new genes with roles in isoprenoid production. Metab. Eng. 15, 174–183.

Redding-Johanson, A.M., Batth, T.S., Chan, R., Krupa, R., Szmidt, H.L., Adams, P.D., Keasling, J.D., Lee, T.S., Mukhopadhyay, A., Petzold, C.J., 2011. Targeted proteomics for metabolic pathway optimization: application to terpene production. Metab. Eng. 13, 194–203.

Reiling, K.K., Yoshikuni, Y., Martin, V.J., Newman, J., Bohlmann, J., Keasling, J.D., 2004. Mono and diterpene production in *Escherichia coli*. Biotechnol. Bioeng. 87, 200–212.

Rohdich, F., Hecht, S., Gartner, K., Adam, P., Krieger, C., Amslinger, S., Arigoni, D., Bacher, A., Eisenreich, W., 2002. Studies on the nonmevalonate terpene biosynthetic pathway: metabolic role of IspH (LytB) protein. Proc. Natl. Acad. Sci. USA 99, 1158–1163.

Sallaud, C., Rontein, D., Onillon, S., Jabes, F., Duffe, P., Giacalone, C., Thoraval, S., Escoffier, C., Herbette, G., Leonhardt, N., Causse, M., Tissier, A., 2009. A novel pathway for sesquiterpene biosynthesis from Z,Z-farnesyl pyrophosphate in the wild tomato Solanum habrochaites. Plant Cell 21, 301–317.

Sambrook, J., Russell, D. (Eds.), 2001. Molecular Cloning: A Laboratory Manual. Cold Spring Harbor Laboratory Press, New York.

Scalcinati, G., Knuf, C., Partow, S., Chen, Y., Maury, J., Schalk, M., Daviet, L., Nielsen, J., Siewers, V., 2012. Dynamic control of gene expression in Saccharomyces cerevisiae engineered for the production of plant sesquitepene alpha-santalene in a fed-batch mode. Metab. Eng. 14, 91–103.

Schulbach, M.C., Brennan, P.J., Crick, D.C., 2000. Identification of a short (C15) chain Z-isoprenyl diphosphate synthase and a homologous long (C50) chain isoprenyl diphosphate synthase in *Mycobacterium tuberculosis*. J. Biol. Chem. 275, 22876–22881.

Schulbach, M.C., Mahapatra, S., Macchia, M., Barontini, S., Papi, C., Minutolo, F., Bertini, S., Brennan, P.J., Crick, D.C., 2001. Purification, enzymatic characterization, and inhibition of the Z-farnesyl diphosphate synthase from *Mycobacterium tuberculosis*. J. Biol. Chem. 276, 11624–11630.

Thulasiram, H.V., Erickson, H.K., Poulter, C.D., 2007. Chimeras of two isoprenoid synthases catalyze all four coupling reactions in isoprenoid biosynthesis. Science 316, 73–76.

Touze, T., Blanot, D., Mengin-Lecreulx, D., 2008. Substrate specificity and membrane topology of *Escherichia coli* PgpB, an undecaprenyl pyrophosphate phosphatase. J. Biol. Chem. 283, 16573–16583.

Wang, C., Kim, J.-Y., Choi, E.-S., Kim, S.-W., 2011a. Microbial production of farnesol (FOH): Current states and beyond. Process Biochem. 46, 1221–1229.

Wang, C., Yoon, S.H., Jang, H.J., Chung, Y.R., Kim, J.Y., Choi, E.S., Kim, S.W., 2011b. Metabolic engineering of *Escherichia coli* for alpha-farnesene production. Metab. Eng. 13, 648–655.

Wang, C., Yoon, S.H., Shah, A.A., Chung, Y.R., Kim, J.Y., Choi, E.S., Keasling, J.D., Kim, S.W., 2010. Farnesol production from *Escherichia coli* by harnessing the exogenous mevalonate pathway. Biotechnol. Bioeng. 107, 421–429.

Wang, W., Dong, C., McNeil, M., Kaur, D., Mahapatra, S., Crick, D.C., Naismith, J.H., 2008. The structural basis of chain length control in Rv1086. J. Mol. Biol. 381, 129–140.

Yoon, S.H., Lee, S.H., Das, A., Ryu, H.K., Jang, H.J., Kim, J.Y., Oh, D.K., Keasling, J.D., Kim, S.W., 2009. Combinatorial expression of bacterial whole mevalonate pathway for the production of beta-carotene in *E. coli*. J. Biotechnol. 140, 218–226.

Yoon, S.H., Lee, Y.M., Kim, J.E., Lee, S.H., Lee, J.H., Kim, J.Y., Jung, K.H., Shin, Y.C., Keasling, J.D., Kim, S.W., 2006. Enhanced lycopene production in *Escherichia coli* engineered to synthesize isopentenyl diphosphate and dimethylallyl diphosphate from mevalonate. Biotechnol. Bioeng. 94, 1025–1032.

Yu, J.S., Kleckley, T.S., Wiemer, D.F., 2005. Synthesis of farnesol isomers via a modified Wittig procedure. Org. Lett. 7, 4803–4806.

Zhang, D., Jennings, S.M., Robinson, G.W., Poulter, C.D., 1993. Yeast squalene synthase: expression, purification, and characterization of soluble recombinant enzyme. Arch. Biochem. Biophys. 304, 133–143.